

CoMoVi: Co-Generation of 3D Human Motions and Realistic Videos

Chengfeng Zhao¹ Jiazhi Shu² Yubo Zhao¹ Tianyu Huang³ Jiahao Lu¹
 Zekai Gu¹ Chengwei Ren¹ Zhiyang Dou⁴ Qing Shuai⁵ Yuan Liu¹ \square
¹HKUST ²SCUT ³CUHK ⁴MIT ⁵ZJU

{chengfeng.zhao@connect.ust.hk, yuanly@ust.hk}

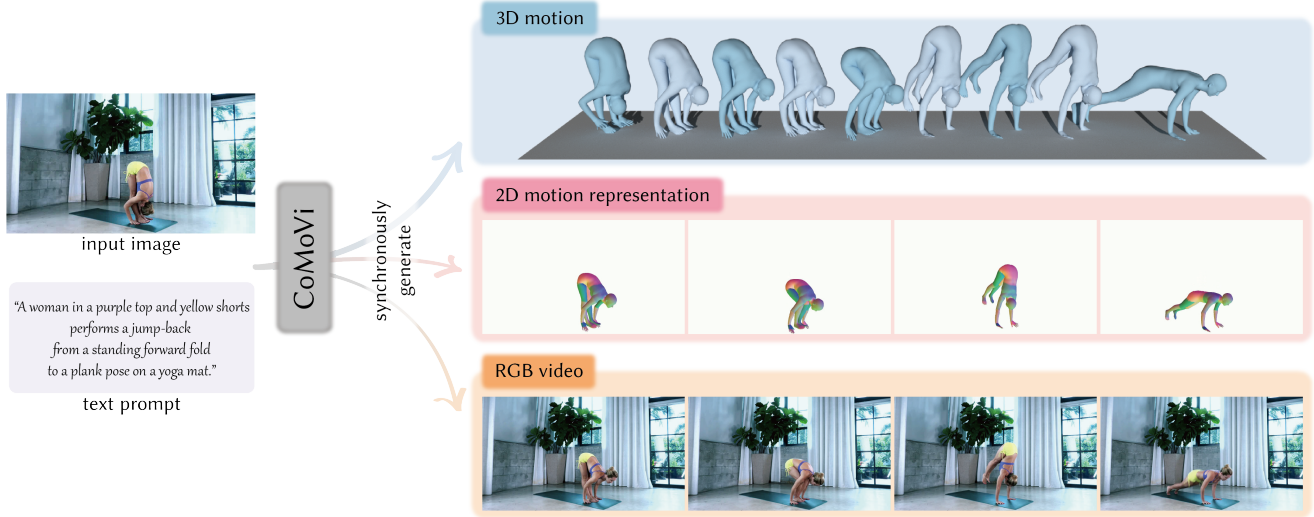


Figure 1. Given an input human image and motion description, **CoMoVi** generates 3D human motion and realistic video synchronously.

Abstract

*In this paper, we find that the generation of 3D human motions and 2D human videos is intrinsically coupled. 3D motions provide the structural prior for plausibility and consistency in videos, while pre-trained video models offer strong generalization capabilities for motions, which necessitate coupling their generation processes. Based on this, we present **CoMoVi**, a co-generative framework that couples two video diffusion models (VDMs) to generate 3D human motions and videos synchronously within a single diffusion denoising loop. To achieve this, we first propose an effective 2D human motion representation that can inherit the powerful prior of pre-trained VDMs. Then, we design a dual-branch diffusion model to couple human motion and video generation process with mutual feature interaction and 3D-2D cross attentions. Moreover, we curate **CoMoVi Dataset**, a large-scale real-world human video dataset with text and motion annotations, covering diverse and challenging human motions. Extensive experiments demonstrate the effectiveness of our method in both 3D human motion and video generation tasks. Our code and data will be released at our [project page](#).*

1. Introduction

The generation of 3D human motion and realistic video sequences is essential to understanding human behaviors and coherent visual dynamics, with broad downstream applications including character animation, VR/AR, and gaming.

High-fidelity human video generation is critically dependent on 3D human motion priors. Although recent VDMs [1, 5, 26, 85, 108] demonstrate remarkable performance and strong generalization capabilities, the generation of a video about a specific person performing a particular action with high fidelity remains challenging. To address this, many works incorporate 3D human motion as driving signals to guide the video generation process [18, 23, 27, 62, 80, 112, 115, 116, 118] via ControlNet-like architecture [110]. Utilizing such 3D priors offers a two-fold advantage: (i.) it enhances controllability, allowing for precise specification of the desired poses; (ii.) it incorporates the inherent human body structure. The semantic and structural priors help guide VDMs in producing more anatomically plausible and natural-looking human figures, which is often a challenge for prior-free models. Consequently, the key challenge lies in how to obtain high-quality 3D human motion data effectively and reliably.

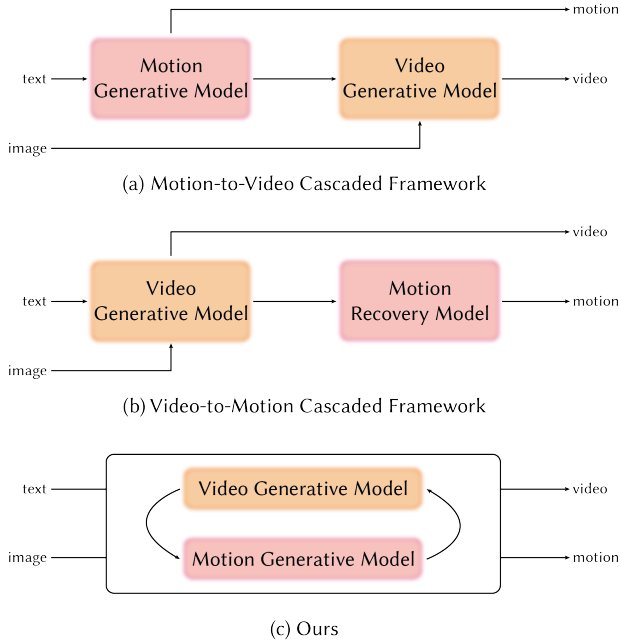


Figure 2. Different paradigms of motion video co-generation.

Traditionally, text-driven motion generation models can generate 3D human motion given textual descriptions [2, 14, 16, 17, 21, 24, 25, 34, 41, 60, 84, 96, 101, 109, 111, 117]. However, these models are often constrained by the bottleneck of high-quality 3D motion data, leading to limited generalization capabilities and low prompt fidelity. Recently, advanced approaches attempt to overcome these limitations by first utilizing VDMs to generate human videos and then applying video-based motion capture algorithms to recover 3D human motion [31, 49, 68]. While VDMs generalize well, they often struggle with highly structured objects such as human bodies, frequently producing implausible motions with inconsistent body structure, which in turn corrupts the recovered 3D motion.

Through our discussion above, it is revealed that there exists a strong coupling relationship between 3D human motion and video generation. High-quality 3D motion can derive high-fidelity generated videos, and reversely, the powerful prior of VDMs can enhance the generalization capabilities of 3D motion generation. However, as illustrated in Fig. 2, existing works are cascaded, either in a motion-to-video or a video-to-motion framework, which are suboptimal. In this paper, we introduce **CoMoVi**, a novel framework for the co-generation of 3D human motion and human video synchronously. This co-generative framework allows mutual information exchange between the motion and video generation processes, enabling generalization enhancement for motion generation and structure guidance for video generation concurrently.

Specifically, **CoMoVi** takes an input image with a text description and generates 3D human motion and video se-

quence synchronously within a single diffusion denoising loop. We first propose a simple yet effective 2D human motion representation that compresses 3D human motion information into pixel space, which directly inherits temporal coherence and denoising behavior from pretrained VDMs. Then, we design a dual-branch diffusion model extended from Wan2.2-I2V-5B [85] to couple the denoising process of 2D motion videos and RGB videos with mutual feature interactions, making video generation aware of 3D human priors. Furthermore, we insert 3D-2D cross-attention modules between each diffusion block to generate 3D human motion from features fused by 2D motion and RGB video latents, propagating the prior of pre-trained VDMs to 3D motion generation. For our model training and evaluation, we curate a large-scale and high-quality dataset called **CoMoVi Dataset** which contains around 50K high-resolution real-world human videos with well-annotated text and motion labels, covering diverse and challenging human motions.

To demonstrate the effectiveness of **CoMoVi**, we conduct comprehensive experiments on the Motion-X++ dataset [48], VBench benchmark [29, 30, 114], and our **CoMoVi Dataset** for both motion generation and video generation tasks. Qualitative and quantitative results validate that our approach is effective in generalizable 3D human motion generation and realistic human video generation concurrently, outperforming state-of-the-art text-to-motion (T2M) and image-to-video (I2V) models.

2. Related Works

Text-driven Human Motion Synthesis. Along with the emergence of large-scale human motion datasets with natural language labels [4, 8, 10, 17, 20, 48, 57–59, 69, 70, 73, 83, 91, 92, 97], T2M methods step a lot forward in both diffusion [14, 16, 41, 60, 84, 111, 117] and autoregressive directions [2, 21, 25, 34, 98, 101, 109]. However, the scarcity of high-quality 3D motion data constrains their diversity and generalization capabilities. To overcome this limitation, recent works leverage multi-view diffusion models [7, 13, 32, 53] to generate 2D motion sequences and then triangulate to 3D [31, 68]. Though effective, these approaches separate 2D generation and 3D reconstruction into two independent processes and only consider human motion as 2D joint coordinates, neglecting the coupling relationship between 3D motion and 2D frames. Our work proposes to encode 3D motion into the same space pre-trained VDMs [1, 5, 26, 39, 85, 108] to generate 3D motion and 2D video synchronously.

Image-based Human Animation. Based on powerful image generation, pioneering image animation works animate static images by fine-tuning or adding additional motion adapters [22, 37] to pre-trained text-to-image (T2I) models [75]. Inspired by the success of ControlNet [110], a

series of motion-driven methods are developed, utilizing 2D pose [107] to drive human video generation [18, 27, 62, 80, 112]. Recent works incorporate more multimodal control signals such as 3D parametric body model [23, 54, 67, 76, 115, 116, 118], camera trajectory [43, 77, 93], optical flow [47, 78], 3D scene geometry [9, 19], novel background [44, 46, 63, 64], and audio [12, 33, 95] to empower multi-subject interaction animation [89, 94], video subject replacement [15], and promptable animation [36, 38]. Additionally, researchers also explore how to implicitly transfer high-level motion patterns directly from reference to target videos [3, 79, 81, 82], bypassing the extraction of explicit driving motion signals. Yet, such methods still require extra reference videos to drive the animation and are not capable of co-generating 3D motions and 2D videos.

Joint Generation of Human Motion and Video. In order to achieve co-generation and remove the dependency of driving sources, latest works follow a cascaded generation pipeline by tailoring one generative model to the other. Motion-to-video methods generate human videos conditioning on pre-generated 2D pose [18, 86, 100], 3D motion [28, 45, 52, 61, 87] or optical flow [47] sequences, and video-to-motion frameworks [51] first generate human video and then refine it using the motion estimation results. Nevertheless, cascaded pipelines propagate defects in the upstream model and overlook the coupling relationship of two generative processes. In the field of multimodal generation and understanding, advanced approaches co-generate RGB videos and normals [88, 94, 99], depths [42, 55, 56, 88, 94, 99, 102], segmentations [88, 99], optical flow [11], and motion maps [40]. However, the co-generation of 3D human motions and 2D videos [65, 106] has not been well studied.

3. Method

In this section, we first introduce our 2D human motion representation, which encodes a 3D parametric body model [54, 67, 76] into pixel space. Subsequently, we elaborate on our design of a dual-branch diffusion model called CoMoVi, which is based on Wan2.2-I2V-5B [85] with mutual feature interaction and 3D-2D cross-attention modules. Finally, we present our curated CoMoVi Dataset that contains around 50K real-world human videos annotated with text and motion labels, covering diverse and challenging human poses.

3.1. Overview

Our goal is to co-generate 3D human motion $\{\mathbf{m}_i \in \mathbb{R}^{J \times 3}\}_{i=0}^F$ and video $\{\mathbf{s}_i \in \mathbb{R}^{H \times W \times 3}\}_{i=0}^F$ sequence in F frames given a starting image \mathbf{s}_0 and a text description \mathbf{p} . In which J is the number of body joints defined by SMPL [54], and $H \times W$ is the resolution of

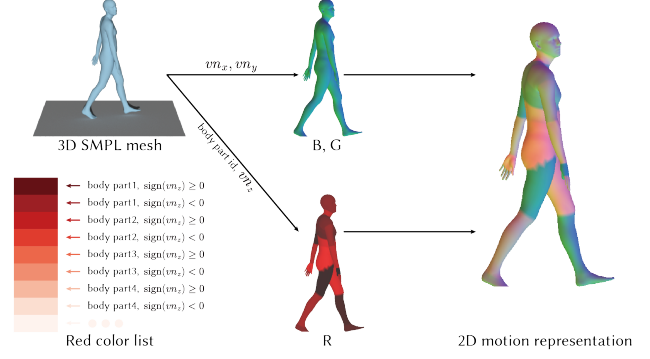


Figure 3. We compress normals and body part semantics of 3D SMPL meshes into RGB images.

generated videos. As illustrated in Fig. 4, we first estimate the 3D human motion \mathbf{m}_0 of \mathbf{s}_0 using CameraHMR [66] and render the 3D SMPL mesh posed in \mathbf{m}_0 as our 2D human motion representation $\mathbf{k}_0 \in \mathbb{R}^{H \times W \times 3}$ according to vertex normals and body part semantics (Sec. 3.2). Then, \mathbf{s}_0 and \mathbf{k}_0 are zero-padded to F frames and fed into each branch of our dual-branch diffusion model, together with \mathbf{m}_0 and \mathbf{p} to generate human video $\{\mathbf{s}_i\}_{i=0}^F$, 2D motion map $\{\mathbf{k}_i\}_{i=0}^F$, and 3D human motion $\{\mathbf{m}_i\}_{i=0}^F$ sequence synchronously (Sec. 3.3). Our training data is prepared as introduced by Sec. 3.4.

3.2. 2D Human Motion Representation

To directly leverage the powerful prior of VDMs and provide 3D human structural feedback, we require a motion representation that satisfies the following properties: (i.) it can be encoded as RGB images; (ii.) it should preserve as much 3D information as possible; (iii.) it should incorporate body part segmentation semantics. Therefore, we propose a color encoding strategy that compresses body surface normals and part semantics of 3D SMPL mesh into RGB channels.

To be specific, given the i -th vertex $\mathbf{v}_e = (v_{ex}, v_{ey}, v_{ez})$ of SMPL mesh, the vertex normal $\mathbf{v}_n = (v_{nx}, v_{ny}, v_{nz})$ satisfies

$$v_{nz} = \pm \sqrt{1 - v_{nx}^2 - v_{ny}^2}, \quad (1)$$

providing that v_{nx} and v_{ny} are known and only $\text{sign}(v_{nz})$ is undetermined. Thus, we can combine this sign with body part semantics and encode both into a single vertex color channel. As illustrated in Fig. 3, we first encode v_{nx} and v_{ny} as the Blue and Green channels, respectively. Then, suppose that SMPL can be segmented into R body parts, we define a color list containing $2R$ candidate values uniformly sampled in the range $[0, 1]$ for the Red channel. The Red channel value for \mathbf{v}_e of part r is assigned as

$$\text{Red}(\mathbf{v}_e) = \begin{cases} \text{RedList}[r] & \text{if } \text{sign}(v_{nz}) \geq 0 \\ \text{RedList}[r+1] & \text{if } \text{sign}(v_{nz}) < 0. \end{cases} \quad (2)$$

This strategy enables effective compression of 3D surface

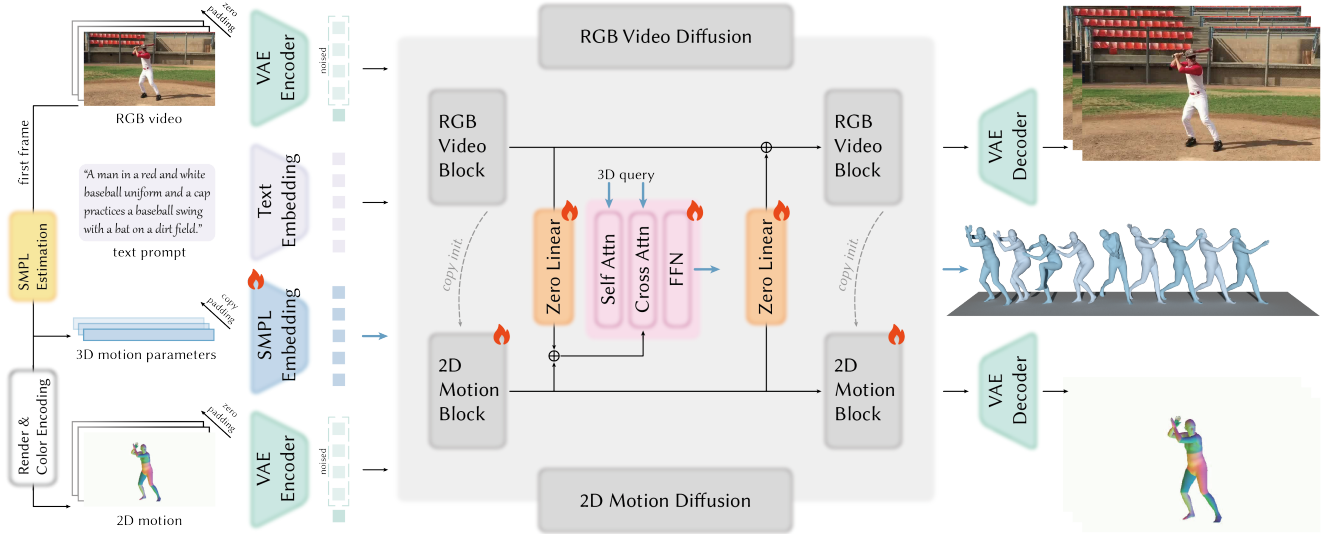


Figure 4. Pipeline overview of CoMoVi. Our method consists of an effective 2D human motion representation (Sec. 3.2) to encode 3D motion information in pixel space, and a dual-branch diffusion model extended from Wan2.2-I2V-5B to coordinate 2D motion and RGB video sequence denoising process with 3D-2D cross-attention modules to concurrently generate 3D human motion (Sec. 3.3).

normals and body part semantics into a single RGB image, which preserves essential 3D structural information and can also be embedded in the latent space of VDMs seamlessly.

3.3. Co-Generation of Human Motion and Video

Previous approaches for multi-modal co-generation, such as VideoJAM [11] and OmniVDiff [99], concatenate multi-modal sequences along the channel dimension and learn a new and joint diffusion latent space. However, we observe that this strategy corrupts the prior of pre-trained VDMs which requires substantial computational resources to reconstruct it (see Sec. 4.5). In contrast, our method adopts a dual-branch diffusion architecture inspired by VACE [35]. Differently, instead of making a distributed copy [35], we make a full copy $\mathcal{D}^{\text{motion}}$ of the diffusion transformer blocks from the pre-trained Wan2.2-I2V-5B $\mathcal{D}^{\text{video}}$ [85] and incorporate mutual feature interactions between the two branches at each block. The reason is distributed copy leads to a complete loss of the prior of pre-trained VDMs, making the training process of $\mathcal{D}^{\text{motion}}$ almost from scratch (see Sec. 4.5).

Adapt Pre-trained VDM to 2D Motion Domain. As shown in Fig. 5, although directly applying the pre-trained VDM to our 2D motion representation sequence can preserve motion semantics, it introduces significant appearance shifts that corrupt the essential color patterns which encompass rich 3D information. Therefore, the first stage of our training is to adapt the weights of $\mathcal{D}^{\text{motion}}$ from the RGB video to our 2D motion representation domain. Specifically, given a 2D motion representation sequence $\{\mathbf{k}_i\}_{i=0}^F$, its clean latent $\mathbf{x}_0^{\text{motion}} \in \mathbb{R}^{C \times (\frac{F-1}{4}+1) \times \frac{H}{16} \times \frac{W}{16}}$ is obtained using the freezed Wan2.2-VAE encoder \mathcal{E} [85]

$$\mathbf{x}_0^{\text{motion}} = \mathcal{E}(\{\mathbf{k}_i\}_{i=0}^F), \quad (3)$$

where C represents the latent dimension of our diffusion model. Then, we add noise ϵ^{motion} according to the denoising step $t \in [0, 1]$ to get

$$\mathbf{x}_t^{\text{motion}} = (1-t)\epsilon^{\text{motion}} + t\mathbf{x}_0^{\text{motion}}. \quad (4)$$

Note that the first frame of $\mathbf{x}_t^{\text{motion}}$ that serves as the generation condition is noise-free. We follow the flow matching training strategy [50] to train $\mathcal{D}^{\text{motion}}$ to learn the velocity field $\mathbf{v}_t^{\text{motion}} = \mathbf{x}_0^{\text{motion}} - \epsilon^{\text{motion}}$ using the objective function

$$\mathcal{L}^{\text{motion}} = \mathbb{E}_{\mathbf{x}_0, \epsilon, \mathbf{p}} \left[\|\mathcal{D}(\mathbf{x}_t, t, \mathbf{p}) - \mathbf{v}_t\|_2^2 \right]. \quad (5)$$

Mutual Feature Interactions. Following the domain adaptation stage, we couple $\mathcal{D}^{\text{motion}}$ with $\mathcal{D}^{\text{video}}$ in training. Distinguished from ControlNet [110] and VACE [35] in which the trainable copy branch provides explicit and clean control signals, our $\mathcal{D}^{\text{motion}}$ participates in a common generation process with $\mathcal{D}^{\text{video}}$ within a single denoising loop. Therefore, our framework requires not only the injection of unidirectional guidance from $\mathcal{D}^{\text{motion}}$ to $\mathcal{D}^{\text{video}}$, but also an effective fusion of latent features of both branches to mutually steer each other toward the denoising direction, which can also benefit 3D motion generation. Concretely, we insert zero-linear modules after the i -th diffusion block to obtain

$$\begin{aligned} \mathbf{x}_t^{\text{fused}} &= \mathbf{x}_t^{\text{motion}} + \text{ZeroLinear}_i(\mathbf{x}_t^{\text{video}}) \\ \mathbf{x}_t^{\text{video}} &= \mathbf{x}_t^{\text{video}} + \text{ZeroLinear}_{i+1}(\mathbf{x}_t^{\text{motion}}), \end{aligned} \quad (6)$$

then pass $\mathbf{x}_t^{\text{motion}}$ and $\mathbf{x}_t^{\text{video}}$ to the $(i+1)$ -th diffusion block of $\mathcal{D}^{\text{motion}}$ and $\mathcal{D}^{\text{video}}$ respectively. The fused latent $\mathbf{x}_t^{\text{fused}}$ will serve as the key and value in our 3D-2D cross-attention module to generate 3D human motion.



Figure 5. We observe that pre-trained VDM results in significant appearance shift on our 2D motion representation, which corrupts the inherent 3D information.

3D-2D Cross-Attention Module. For each diffusion block layer, given the fused latent feature $\mathbf{x}_t^{\text{fused}}$, we design a shared module \mathcal{A} composed of 6 layers of self-attention, cross-attention, and feed-forward network combination to generate 3D human motion sequence $\{\mathbf{m}_i\}_{i=1}^F$ as

$$\{\mathbf{m}_i\}_{i=1}^F = \mathcal{A}(\mathbf{m}_0, \mathbf{x}_t^{\text{fused}}). \quad (7)$$

We describe this process in detail below. We first initialize all F frames’ SMPL poses with the known initial pose \mathbf{m}_0 , and apply a SMPL embedding layer to increase the feature dimension to $\mathbf{q} \in \mathbb{R}^{F \times C}$. Subsequently, these initial pose embeddings are used as 3D queries going through self-attention layers as

$$\mathbf{q} = \text{SelfAttention}(\mathbf{q}). \quad (8)$$

Then \mathbf{q} will interact with $\mathbf{x}_t^{\text{fused}}$ to generate human poses for all frames. Since $\mathbf{x}_t^{\text{fused}}$ is derived from 2D video latents which are compressed along temporal axis by the VAE encoder \mathcal{E} with compression ratio as 4 [85], 1 frame of $\mathbf{x}_t^{\text{fused}}$ corresponds to 4 frames of \mathbf{q} . Therefore, we re-organize \mathbf{q} per 4 frames to get $\mathbf{q}' \in \mathbb{R}^{\frac{F-1}{4} \times 4 \times C}$ and apply 3D-2D cross attention as

$$\mathbf{q}' = \text{CrossAttention}(\mathbf{q}', \mathbf{x}_t^{\text{fused}}). \quad (9)$$

Finally, our model generates 3D human motion $\{\mathbf{m}_i\}_{i=1}^F$ by a feed-forward network and a final output projection layer to map \mathbf{q}' back to SMPL parametric dimension. During training, we tune all trainable modules jointly (see Fig. 4). The total training loss is defined as

$$\mathcal{L} = \mathcal{L}^{\text{motion}} + \mathcal{L}^{\text{video}} + \mathcal{L}^{\text{smpl}}, \quad (10)$$

where $\mathcal{L}^{\text{video}}$ has the same definition as Eq. 5 for RGB video branch, and $\mathcal{L}^{\text{smpl}}$ is formulated as

$$\mathcal{L}^{\text{smpl}} = \frac{1}{F-1} \sum_{i=1}^{F-1} \|\mathbf{m}_i - \text{GT}(\mathbf{m}_i)\|_2^2. \quad (11)$$

3.4. CoMoVi Dataset

Training our co-generative framework requires a high-quality dataset of triplets containing human videos, 3D human motions, and text annotations. As reported in Tab. 1, existing datasets [6, 48, 49, 74, 86, 93, 113] fail to simultaneously meet our demands for high-quality video and sufficient 3D

Dataset	Clips	Motion Type	Resolution
Motion-X++ [48]	120,500	3D SMPL	-
HumanVid* [93]	19,688	2D Pose	1080P+
MotionVid [86]	1.2M	2D Pose	-
ViMoGen-228K* [49]	41,971	3D SMPL	720P+
CoMoVi Dataset	54,053	3D SMPL	720P+

Table 1. Comparison of CoMoVi Dataset with existing datasets. “*”: We only count real-world data.

motion. Therefore, we curate CoMoVi Dataset. We source high-resolution human videos from Koala-36M [90], HumanVid [93], and publicly available Internet videos, and employ a carefully designed filtering pipeline to select clips featuring single-person motion based on Qwen3 [105], Qwen2.5-VL [104] and YOLO [72]. For 3D human motion annotations, we obtain pseudo-labels using CameraHMR [66] followed by a smoothing post-processing procedure. For text descriptions, we utilize Gemini-2.5-Pro to generate precise motion captions for each video. Further details are provided in the supplementary material.

4. Experiments

In this section, we first introduce our implementation and evaluation details. Then, we compare our approach with state-of-the-art T2M and I2V models for motion generation and video generation tasks, respectively. Finally, we conduct ablation studies to validate the effectiveness of our designs.

4.1. Implementation Details

We train our model on the training set of our proposed dataset using 24 A100-SXM4-40G GPUs with per GPU batch size 1 and gradient accumulation steps 4 for 6,000 optimization steps. We use the ZeRO-3 [71] strategy and AdamW optimizer with learning rate 2e-5. Our training data are unified to resolution $H \times W = 704 \times 1280$, $F = 81$ frames in 16 fps. More implementation details can be found in the supplementary material.

4.2. Evaluation Datasets and Metrics

For comprehensive evaluations on both motion generation and video generation tasks, we take the widely-used Motion-X++ dataset [48], VBench benchmark [29, 30, 114], and also our testing set to assess performance of all compared models. For the motion generation task, we adhere to the evaluation protocol defined by MoMask [21] and use Frechet Inception Distance (FID), R-Precision (@1 and @3), and MultiModal Distance (MMDist) metrics. For the video generation task, we calculate all metrics provided by VBench except for “dynamic degree”, which is aimed at measuring scene-level dynamics, on our testing set. For the following tables, the numbers marked in **bold** and underlined represent the first and second best, respectively.

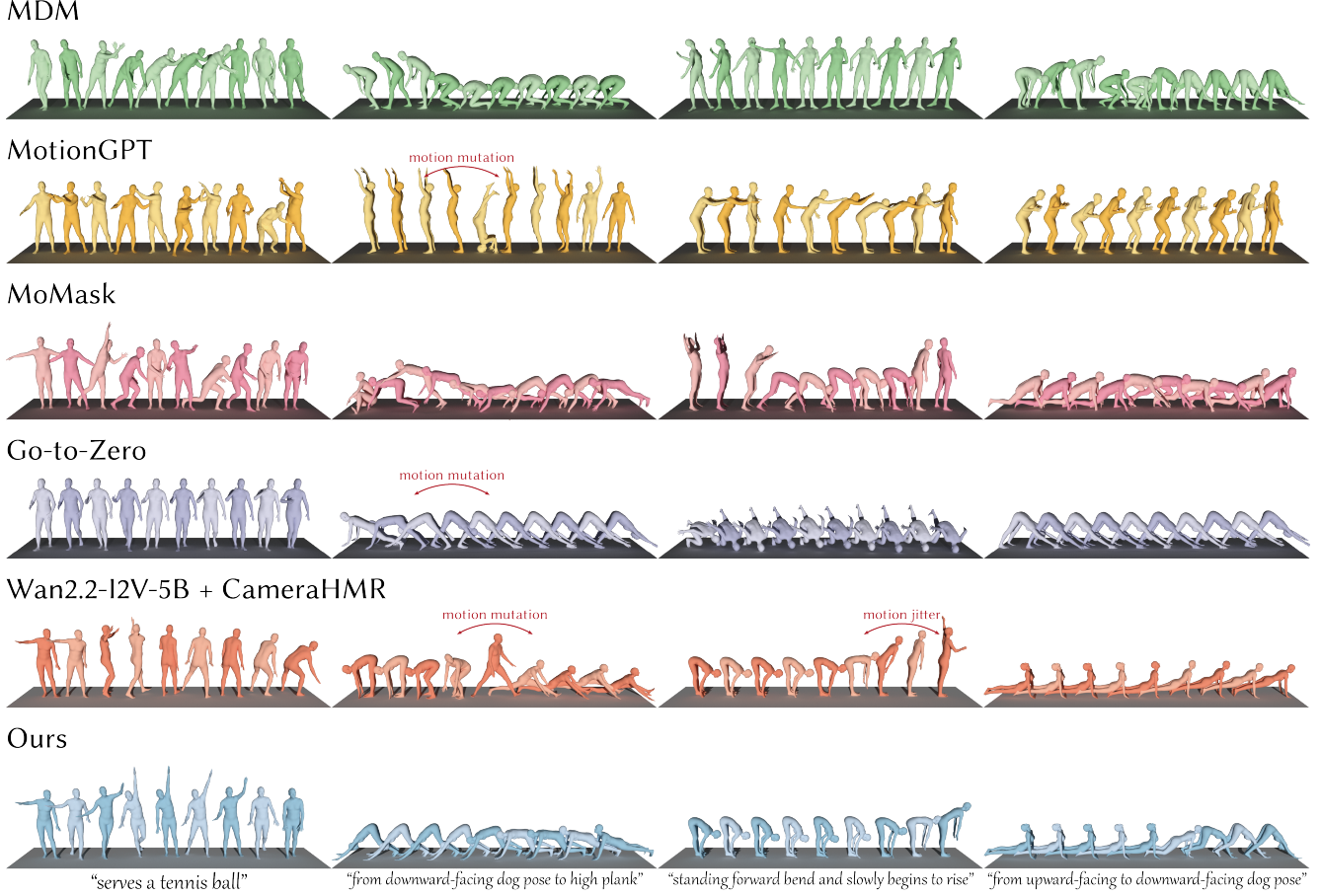


Figure 6. Qualitative comparison of 3D human motion generation with state-of-the-art T2M models [17, 21, 34, 84]. Wan2.2-I2V-5B+CameraHMR [66, 85] is a naive baseline composed a video generation model followed by a video motion capture model. We present motion keywords in text prompts for simplicity.

Method	CoMoVi Dataset				Motion-X++ [48]			
	FID \downarrow	R@1 \uparrow	R@3 \uparrow	MMDist \downarrow	FID \downarrow	R@1 \uparrow	R@3 \uparrow	MMDist \downarrow
MDM [84]	27.740	0.287	0.540	4.848	20.871	0.332	0.406	4.803
MotionGPT [34]	26.079	0.316	0.569	4.486	27.084	0.305	0.529	5.276
MoMask [21]	24.521	0.385	0.606	4.943	19.365	0.316	0.569	4.915
Go-to-Zero-3B* [17]	3.175	0.440	0.605	3.585	<u>15.474</u>	0.311	<u>0.692</u>	3.751
Go-to-Zero-7B* [17]	1.641	0.459	<u>0.608</u>	3.429	14.470	0.384	0.699	<u>3.578</u>
Wan+CameraHMR [66, 85]	<u>0.815</u>	<u>0.539</u>	<u>0.591</u>	<u>3.056</u>	21.538	0.302	0.464	3.735
Ours	0.349	0.565	0.640	3.035	16.728	<u>0.377</u>	0.571	3.507

Table 2. Quantitative evaluation of 3D human motion generation. “*”: Motion-X++ [48] is in the training set of Go-to-Zero [17].

4.3. Comparisons on Motion Generation Task

Baselines. We compare with state-of-the-art T2M methods, including diffusion-based MDM [84] and autoregressive MotionGPT [34], MoMask [21], and Go-to-Zero [17]. Additionally, since no method perfectly matching with our setting is available currently, we build and compare with a naive yet meaningful baseline Wan2.2-I2V-5B+CameraHMR [66, 85] that first generates human video from a starting image and a text prompt, and then captures the 3D motion of the person in that generated video. It is noteworthy that we sample test sequences from Motion-X++ [48] on our own since no

official train/test split is provided, which might be included in the training set of Go-to-Zero [17].

Results. As presented in Fig. 6, CoMoVi generates 3D human motions with high prompt fidelity and dynamic smoothness, while baselines often produce jittery motions, unrelated contents, and implausible body movements. Quantitative evaluations in Tab. 2 also validates that our co-generative framework outperforms state-of-the-art T2M models on testing set of CoMoVi Dataset, and also generalizes well, achieving comparable performance on unseen MotionX++ dataset [48] to Go-to-Zero [17].

CogVideoX1.5-I2V-5B



Wan2.2-I2V-5B



Ours



1st row prompt: "A woman in black and white patterned yoga attire performs the downward-facing dog yoga pose on a white yoga mat."

2nd row prompt: "A woman in black activewear holds her arms behind her, then twists her torso and reaching her arms up towards the ceiling."

Figure 7. Qualitative comparison of human video generation with state-of-the-art open-source I2V models [85, 108].

Method	Subject Consistency ↑	Background Consistency ↑	Motion Smoothness ↑	Aesthetic Quality ↑	Imaging Quality ↑
CogVideoX1.5-I2V-5B [108]	0.933	0.947	0.991	0.512	0.716
Wan2.2-I2V-5B [85]	0.948	0.960	0.993	0.529	0.713
Ours	0.955	0.963	0.993	0.533	0.718

Table 3. Quantitative evaluation of human video generation using VBench metrics [29, 30, 114].

4.4. Comparisons on Video Generation Task

Baselines. We choose to compare with two leading open-source I2V models, CogVideoX1.5-I2V-5B [108] and Wan2.2-I2V-5B [85], to which the model size of CoMoVi is comparable. This selection ensures a fair and meaningful comparison between models of similar scale and capability.

Results. As depicted in Fig. 7, CoMoVi gets benefits from our 2D motion representation which encapsulates rich 3D motion information, generating realistic human videos with more consistent body structure, higher prompt fidelity, and anatomically plausible motions. While CogVideoX1.5 [108]

and Wan2.2-I2V-5B [85] struggle in motion-prompt misalignment, distorted body shapes, and background maintenance. The quantitative results detailed in Tab. 3 demonstrate the advantage of our co-generative framework in all evaluation dimensions defined by VBench [29, 30, 114].

4.5. Ablation Study

We further conduct extensive ablation studies to validate the significance of our 2D motion representation and the effectiveness of our model architecture design.

Different 2D Motion Representations. As introduced in Sec. 3.2, our 2D human motion representation integrates

Motion Representation / Architecture	Motion Generation				Video Generation				
	FID \downarrow	R@1 \uparrow	R@3 \uparrow	MMDist \downarrow	SC \uparrow	BC \uparrow	MS \uparrow	AQ \uparrow	IQ \uparrow
w/o motion	0.758	0.458	0.556	4.079	0.937	0.944	0.980	0.520	0.709
Normal only	<u>0.415</u>	<u>0.538</u>	<u>0.556</u>	3.003	0.918	0.946	0.988	0.521	0.710
Body semantic only	0.553	0.499	<u>0.589</u>	3.536	<u>0.940</u>	0.944	0.994	0.528	0.708
DWPose [107]	0.503	0.464	0.551	3.396	0.929	0.951	0.981	0.522	0.701
VideoJAM joint latent space	0.755	0.459	0.559	3.534	0.868	0.942	0.987	0.529	0.705
VACE distributed copy	0.625	0.500	0.572	3.148	0.927	0.949	0.994	0.522	0.715
Pass $\mathbf{x}_t^{\text{fused}}$ to $\mathcal{D}^{\text{motion}}$	0.718	0.466	0.552	4.157	0.911	<u>0.955</u>	0.985	<u>0.530</u>	<u>0.718</u>
Ours	0.349	0.565	0.640	<u>3.035</u>	0.955	0.963	<u>0.993</u>	0.533	0.718

Table 4. Quantitative performance evaluation of different motion representations and model architectures.

surface normals with body part semantics. Therefore, we experiment with “normal only” and “body semantic only” settings, and also a commonly used 2D pose representation “DWPose” [107]. Tab. 4 shows that directly fine-tuning Wan2.2-I2V-5B [85] on RGB videos only without our co-generative framework (“w/o motion”) leads to significant performance degradation. While the absence of any factor among normals, body semantics, and surface rendering results in suboptimal performance in both generation tasks.

Different Model Architecture Designs. In designing our model architecture, we explore several approaches inspired by VideoJAM [11] and VACE [35], ultimately adopting a dual-branch diffusion model with the full copy strategy. Specifically, we first refer to VideoJAM [11] to concatenate RGB videos and our 2D motion representations along the latent channel dimension, and double the dimension of the patch embedding layer and the output head layer of Wan2.2-I2V-5B [85]. However, we observe that this severely disrupts the pre-trained VDM’s latent space during the initial training phase, necessitating a slow and computationally expensive reconstruction process. Consequently, this method fails to outperform even the baseline models with a limited training budget. Therefore, we adopt dual-branch diffusion architecture following VACE [35], which effectively preserves the integrity of the latent space of pre-trained VDM. Nevertheless, we identify that the distributed copy strategy proposed by VACE [35] causes the copied branch to completely lose the prior knowledge of pre-trained VDM. At the first training step, the output of the copied branch is totally noised, indicating that it essentially discards priors and requires to be trained from scratch. The quantitative performance shown in Tab. 4 demonstrates that our dual-branch diffusion architecture with the full copy strategy achieves better performance in both generation tasks. Furthermore, we experiment with passing the fused latent feature $\mathbf{x}_t^{\text{fused}}$ defined in Eq. 6 rather than $\mathbf{x}_t^{\text{motion}}$ to the 2D motion diffusion branch $\mathcal{D}^{\text{motion}}$. Intriguingly, it is found that the direct feature injection from RGB to 2D motion latents significantly disturbs the denoising process of $\mathcal{D}^{\text{motion}}$. We analyze that 2D motion representation is far more sparse than RGB videos containing rich appearances and background details, which results in chaotic

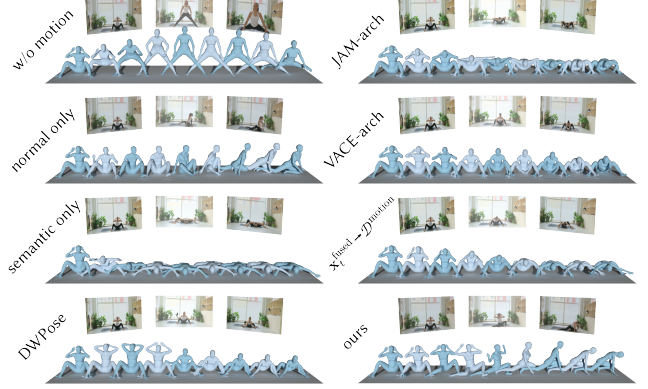


Figure 8. Qualitative results of different motion representations and model architectures. The input motion keyword is: “transition from seated state to get up and stretch body”.

and fluctuating artifacts in 2D motion generation, degrading the preservation of essential 3D information. And eventually, the effectiveness of motion guidance is weakened, leading to the suboptimal performance (see Fig. 8).

5. Conclusion

In this work, we propose a novel framework called CoMoVi for co-generation of 3D human motions and realistic videos. Our key idea is to couple the denoising process of 3D motions and 2D videos, enabling synchronous generation of both within a single diffusion loop. We first introduce a novel 2D motion representation that encodes surface normals and body part semantics of 3D SMPL mesh into RGB images, allowing it to directly inherit priors from pre-trained VDMs. Then, we develop a dual-branch diffusion model with mutual feature interactions and 3D-2D cross-attentions, providing motion guidance for video generation while propagating VDM’s generalization capability to 3D motion generation. Moreover, we contribute the CoMoVi Dataset, a large-scale human video collection annotated with high-quality text and motion labels to support versatile video-based and motion-related tasks. Comprehensive experiments on multiple benchmarks demonstrate our method’s effectiveness in both motion and video generation.

References

- [1] Niket Agarwal, Arslan Ali, Maciej Bala, Yogesh Balaji, Erik Barker, Tiffany Cai, Prithvijit Chattopadhyay, Yongxin Chen, Yin Cui, Yifan Ding, et al. Cosmos world foundation model platform for physical ai. *arXiv preprint arXiv:2501.03575*, 2025. 1, 2
- [2] Hyemin Ahn, Timothy Ha, Yunho Choi, Hwiyeon Yoo, and Songhwai Oh. Text2action: Generative adversarial synthesis from language to action. In *2018 IEEE International Conference on Robotics and Automation (ICRA)*, pages 5915–5920. IEEE, 2018. 2
- [3] Yuxuan Bian, Xin Chen, Zenan Li, Tiancheng Zhi, Shen Sang, Linjie Luo, and Qiang Xu. Video-as-prompt: Unified semantic control for video generation. *arXiv preprint arXiv:2510.20888*, 2025. 3
- [4] Michael J Black, Priyanka Patel, Joachim Tesch, and Jinlong Yang. Bedlam: A synthetic dataset of bodies exhibiting detailed lifelike animated motion. In *Proceedings of the IEEE/CVF Conference on Computer Vision and Pattern Recognition*, pages 8726–8737, 2023. 2
- [5] Andreas Blattmann, Tim Dockhorn, Sumith Kulal, Daniel Mendelevitch, Maciej Kilian, Dominik Lorenz, Yam Levi, Zion English, Vikram Voleti, Adam Letts, et al. Stable video diffusion: Scaling latent video diffusion models to large datasets. *arXiv preprint arXiv:2311.15127*, 2023. 1, 2
- [6] Emanuele Bugliarello, Anurag Arnab, Roni Paiss, Pieter-Jan Kindermans, and Cordelia Schmid. What are you doing? a closer look at controllable human video generation. *arXiv preprint arXiv:2503.04666*, 2025. 5
- [7] Zeyu Cai, Ziyang Li, Xiaoben Li, Boqian Li, Zeyu Wang, Zhenyu Zhang, and Yuliang Xiu. Up2you: Fast reconstruction of yourself from unconstrained photo collections. *arXiv preprint arXiv:2509.24817*, 2025. 2
- [8] Bin Cao, Sipeng Zheng, Ye Wang, Lujie Xia, Qianshan Wei, Qin Jin, Jing Liu, and Zongqing Lu. Being-m0. 5: A real-time controllable vision-language-motion model. *arXiv preprint arXiv:2508.07863*, 2025. 2
- [9] Chenjie Cao, Jingkai Zhou, Shikai Li, Jingyun Liang, Chaohui Yu, Fan Wang, Xiangyang Xue, and Yanwei Fu. Uni3c: Unifying precisely 3d-enhanced camera and human motion controls for video generation. *arXiv preprint arXiv:2504.14899*, 2025. 3
- [10] Yukang Cao, Jiahao Lu, Zhisheng Huang, Zhiwen Shen, Chengfeng Zhao, Fangzhou Hong, Zhaoxi Chen, Xin Li, Wenping Wang, Yuan Liu, et al. Reconstructing 4d spatial intelligence: A survey. *arXiv preprint arXiv:2507.21045*, 2025. 2
- [11] Hila Chefer, Uriel Singer, Amit Zohar, Yuval Kirstain, Adam Polyak, Yaniv Taigman, Lior Wolf, and Shelly Sheynin. Videojam: Joint appearance-motion representations for enhanced motion generation in video models. *arXiv preprint arXiv:2502.02492*, 2025. 3, 4, 8
- [12] Liyang Chen, Tianxiang Ma, Jiawei Liu, Bingchuan Li, Zhiwei Chen, Lijie Liu, Xu He, Gen Li, Qian He, and Zhiyong Wu. Humo: Human-centric video generation via collaborative multi-modal conditioning. *arXiv preprint arXiv:2509.08519*, 2025. 3
- [13] Wenyue Chen, Peng Li, Wangguandong Zheng, Chengfeng Zhao, Mengfei Li, Yaolong Zhu, Zhiyang Dou, Ronggang Wang, and Yuan Liu. Synchuman: Synchronizing 2d and 3d generative models for single-view human reconstruction. *arXiv preprint arXiv:2510.07723*, 2025. 2
- [14] Xin Chen, Biao Jiang, Wen Liu, Zilong Huang, Bin Fu, Tao Chen, and Gang Yu. Executing your commands via motion diffusion in latent space. In *Proceedings of the IEEE/CVF conference on computer vision and pattern recognition*, pages 18000–18010, 2023. 2
- [15] Gang Cheng, Xin Gao, Li Hu, Siqi Hu, Mingyang Huang, Chaonan Ji, Ju Li, Dechao Meng, Jinwei Qi, Pengchong Qiao, et al. Wan-animate: Unified character animation and replacement with holistic replication. *arXiv preprint arXiv:2509.14055*, 2025. 3
- [16] Wenxun Dai, Ling-Hao Chen, Jingbo Wang, Jinpeng Liu, Bo Dai, and Yansong Tang. Motionlcm: Real-time controllable motion generation via latent consistency model. In *European Conference on Computer Vision*, pages 390–408. Springer, 2024. 2
- [17] Ke Fan, Shunlin Lu, Minyue Dai, Runyi Yu, Lixing Xiao, Zhiyang Dou, Junting Dong, Lizhuang Ma, and Jingbo Wang. Go to zero: Towards zero-shot motion generation with million-scale data. In *Proceedings of the IEEE/CVF International Conference on Computer Vision*, pages 13336–13348, 2025. 2, 6
- [18] Qijun Gan, Yi Ren, Chen Zhang, Zhenhui Ye, Pan Xie, Xiang Yin, Zehuan Yuan, Bingyue Peng, and Jianke Zhu. Humandit: Pose-guided diffusion transformer for long-form human motion video generation. *arXiv preprint arXiv:2502.04847*, 2025. 1, 3
- [19] Zekai Gu, Rui Yan, Jiahao Lu, Peng Li, Zhiyang Dou, Chenyang Si, Zhen Dong, Qifeng Liu, Cheng Lin, Ziwei Liu, et al. Diffusion as shader: 3d-aware video diffusion for versatile video generation control. In *Proceedings of the Special Interest Group on Computer Graphics and Interactive Techniques Conference Conference Papers*, pages 1–12, 2025. 3
- [20] Chuan Guo, Shihao Zou, Xinxin Zuo, Sen Wang, Wei Ji, Xingyu Li, and Li Cheng. Generating diverse and natural 3d human motions from text. In *Proceedings of the IEEE/CVF conference on computer vision and pattern recognition*, pages 5152–5161, 2022. 2, 1
- [21] Chuan Guo, Yuxuan Mu, Muhammad Gohar Javed, Sen Wang, and Li Cheng. Momask: Generative masked modeling of 3d human motions. In *Proceedings of the IEEE/CVF Conference on Computer Vision and Pattern Recognition*, pages 1900–1910, 2024. 2, 5, 6
- [22] Yuwei Guo, Ceyuan Yang, Anyi Rao, Zhengyang Liang, Yaohui Wang, Yu Qiao, Maneesh Agrawala, Dahua Lin, and Bo Dai. Animatediff: Animate your personalized text-to-image diffusion models without specific tuning. *arXiv preprint arXiv:2307.04725*, 2023. 2
- [23] Jingxuan He, Busheng Su, and Finn Wong. Posegen: In-context lora finetuning for pose-controllable long human video generation. *arXiv preprint arXiv:2508.05091*, 2025. 1, 3

[24] Yannan He, Garvita Tiwari, Tolga Birdal, Jan Eric Lenssen, and Gerard Pons-Moll. Nrdf: Neural riemannian distance fields for learning articulated pose priors. In *Proceedings of the IEEE/CVF Conference on Computer Vision and Pattern Recognition*, pages 1661–1671, 2024. 2

[25] Yannan He, Garvita Tiwari, Xiaohan Zhang, Pankaj Bora, Tolga Birdal, Jan Eric Lenssen, and Gerard Pons-Moll. Molingo: Motion-language alignment for text-to-motion generation. *arXiv preprint arXiv:2512.13840*, 2025. 2

[26] Wenyi Hong, Ming Ding, Wendi Zheng, Xinghan Liu, and Jie Tang. Cogvideo: Large-scale pretraining for text-to-video generation via transformers. *arXiv preprint arXiv:2205.15868*, 2022. 1, 2

[27] Li Hu. Animate anyone: Consistent and controllable image-to-video synthesis for character animation. In *Proceedings of the IEEE/CVF Conference on Computer Vision and Pattern Recognition*, pages 8153–8163, 2024. 1, 3

[28] Hsin-Ping Huang, Yang Zhou, Jui-Hsien Wang, Difan Liu, Feng Liu, Ming-Hsuan Yang, and Zhan Xu. Move-in-2d: 2d-conditioned human motion generation. In *Proceedings of the Computer Vision and Pattern Recognition Conference*, pages 22766–22775, 2025. 3

[29] Ziqi Huang, Yinan He, Jiashuo Yu, Fan Zhang, Chenyang Si, Yuming Jiang, Yuanhan Zhang, Tianxing Wu, Qingyang Jin, Nattapol Chanpaisit, Yaohui Wang, Xinyuan Chen, Limin Wang, Dahua Lin, Yu Qiao, and Ziwei Liu. Vbench: Comprehensive benchmark suite for video generative models. In *Proceedings of the IEEE/CVF Conference on Computer Vision and Pattern Recognition*, 2024. 2, 5, 7

[30] Ziqi Huang, Fan Zhang, Xiaojie Xu, Yinan He, Jiashuo Yu, Ziyue Dong, Qianli Ma, Nattapol Chanpaisit, Chenyang Si, Yuming Jiang, Yaohui Wang, Xinyuan Chen, Ying-Cong Chen, Limin Wang, Dahua Lin, Yu Qiao, and Ziwei Liu. Vbench++: Comprehensive and versatile benchmark suite for video generative models. *arXiv preprint arXiv:2411.13503*, 2024. 2, 5, 7

[31] Zehuan Huang, Haoran Feng, Yangtian Sun, Yuanchen Guo, Yanpei Cao, and Lu Sheng. Animax: Animating the inanimate in 3d with joint video-pose diffusion models. *arXiv preprint arXiv:2506.19851*, 2025. 2

[32] Zehuan Huang, Yuan-Chen Guo, Haoran Wang, Ran Yi, Lizhuang Ma, Yan-Pei Cao, and Lu Sheng. Mv-adapter: Multi-view consistent image generation made easy. In *Proceedings of the IEEE/CVF International Conference on Computer Vision*, pages 16377–16387, 2025. 2

[33] Ziyao Huang, Zixiang Zhou, Juan Cao, Yifeng Ma, Yi Chen, Zejing Rao, Zhiyong Xu, Hongmei Wang, Qin Lin, Yuan Zhou, et al. Hunyuandvideo-homa: Generic human-object interaction in multimodal driven human animation. *arXiv preprint arXiv:2506.08797*, 2025. 3

[34] Biao Jiang, Xin Chen, Wen Liu, Jingyi Yu, Gang Yu, and Tao Chen. Motiogpt: Human motion as a foreign language. *Advances in Neural Information Processing Systems*, 36: 20067–20079, 2023. 2, 6

[35] Zeyinzi Jiang, Zhen Han, Chaojie Mao, Jingfeng Zhang, Yulin Pan, and Yu Liu. Vace: All-in-one video creation and editing. *arXiv preprint arXiv:2503.07598*, 2025. 4, 8

[36] Siyoon Jin, Seongchan Kim, Dahyun Chung, Jaeho Lee, Hyunwook Choi, Jisu Nam, Jiyoung Kim, and Seungryong Kim. Matrix: Mask track alignment for interaction-aware video generation. *arXiv preprint arXiv:2510.07310*, 2025. 3

[37] Johanna Karras, Aleksander Holynski, Ting-Chun Wang, and Ira Kemelmacher-Shlizerman. Dreampose: Fashion image-to-video synthesis via stable diffusion. In *2023 IEEE/CVF International Conference on Computer Vision (ICCV)*, pages 22623–22633. IEEE, 2023. 2

[38] Taeksoo Kim and Hanbyul Joo. Target-aware video diffusion models. *arXiv preprint arXiv:2503.18950*, 2025. 3

[39] Weijie Kong, Qi Tian, Zijian Zhang, Rox Min, Zuozhuo Dai, Jin Zhou, Jiangfeng Xiong, Xin Li, Bo Wu, Jianwei Zhang, et al. Hunyuandvideo: A systematic framework for large video generative models. *arXiv preprint arXiv:2412.03603*, 2024. 2

[40] Jiahui Lei, Kyle Genova, George Kopanas, Noah Snavely, and Leonidas Guibas. Momaps: Semantics-aware scene motion generation with motion maps. In *Proceedings of the IEEE/CVF International Conference on Computer Vision*, pages 10022–10031, 2025. 3

[41] Chuqiao Li, Julian Chibane, Yannan He, Naama Pearl, Andreas Geiger, and Gerard Pons-Moll. Unimotion: Unifying 3d human motion synthesis and understanding. In *2025 International Conference on 3D Vision (3DV)*, pages 240–249. IEEE, 2025. 2

[42] Mengfei Li, Peng Li, Zheng Zhang, Jiahao Lu, Chengfeng Zhao, Wei Xue, Qifeng Liu, Sida Peng, Wenxiao Zhang, Wenhan Luo, Yuan Liu, and Yike Guo. Unish: Unifying scene and human reconstruction in a feed-forward pass. *arXiv preprint arXiv:2601.01222*, 2026. 3

[43] Ruineng Li, Daitao Xing, Huiming Sun, Yuanzhou Ha, Jinglin Shen, and Chiuman Ho. Tokenmotion: Decoupled motion control via token disentanglement for human-centric video generation. In *Proceedings of the Computer Vision and Pattern Recognition Conference*, pages 1951–1961, 2025. 3

[44] Weiqi Li, Zehao Zhang, Liang Lin, and Guangrun Wang. Humangenesis: Agent-based geometric and generative modeling for synthetic human dynamics. *arXiv preprint arXiv:2508.09858*, 2025. 3

[45] Zekun Li, Rui Zhou, Rahul Sajnani, Xiaoyan Cong, Daniel Ritchie, and Srinath Sridhar. Genhs: Controllable generation of human-scene interaction videos. *arXiv preprint arXiv:2506.19840*, 2025. 3

[46] Jingyun Liang, Jingkai Zhou, Shikai Li, Chenjie Cao, Lei Sun, Yichen Qian, Weihua Chen, and Fan Wang. Realismotion: Decomposed human motion control and video generation in the world space. *arXiv preprint arXiv:2508.08588*, 2025. 3

[47] Xinyao Liao, Xianfang Zeng, Liao Wang, Gang Yu, Guosheng Lin, and Chi Zhang. Motionagent: Fine-grained controllable video generation via motion field agent. *arXiv preprint arXiv:2502.03207*, 2025. 3

[48] Jing Lin, Ailing Zeng, Shunlin Lu, Yuanhao Cai, Ruimao Zhang, Haoqian Wang, and Lei Zhang. Motion-x: A large-scale 3d expressive whole-body human motion dataset. *Advances in Neural Information Processing Systems*, 36:25268–25280, 2023. 2, 5, 6

[49] Jing Lin, Ruiqi Wang, Junzhe Lu, Ziqi Huang, Guorui Song, Ailing Zeng, Xian Liu, Chen Wei, Wanqi Yin, Qingping Sun, et al. The quest for generalizable motion generation: Data, model, and evaluation. *arXiv preprint arXiv:2510.26794*, 2025. 2, 5

[50] Yaron Lipman, Ricky TQ Chen, Heli Ben-Hamu, Maximilian Nickel, and Matt Le. Flow matching for generative modeling. *arXiv preprint arXiv:2210.02747*, 2022. 4

[51] Qihao Liu, Ju He, Qihang Yu, Liang-Chieh Chen, and Alan Yuille. Revision: High-quality, low-cost video generation with explicit 3d physics modeling for complex motion and interaction. *arXiv preprint arXiv:2504.21855*, 2025. 3

[52] Shaowei Liu, Chuan Guo, Bing Zhou, and Jian Wang. Ponimotor: Unfolding interactive pose for versatile human-human interaction animation. In *Proceedings of the IEEE/CVF International Conference on Computer Vision*, pages 12068–12077, 2025. 3

[53] Yuan Liu, Cheng Lin, Zijiao Zeng, Xiaoxiao Long, Lingjie Liu, Taku Komura, and Wenping Wang. Syncdreamer: Generating multiview-consistent images from a single-view image. *arXiv preprint arXiv:2309.03453*, 2023. 2

[54] Matthew Loper, Naureen Mahmood, Javier Romero, Gerard Pons-Moll, and Michael J Black. Smpl: A skinned multi-person linear model. In *Seminal Graphics Papers: Pushing the Boundaries, Volume 2*, pages 851–866. 2023. 3

[55] Jiahao Lu, Tianyu Huang, Peng Li, Zhiyang Dou, Cheng Lin, Zhiming Cui, Zhen Dong, Sai-Kit Yeung, Wenping Wang, and Yuan Liu. Align3r: Aligned monocular depth estimation for dynamic videos. In *Proceedings of the Computer Vision and Pattern Recognition Conference*, pages 22820–22830, 2025. 3

[56] Jiahao Lu, Weitao Xiong, Jiacheng Deng, Peng Li, Tianyu Huang, Zhiyang Dou, Cheng Lin, Sai-Kit Yeung, and Yuan Liu. Trackingworld: World-centric monocular 3d tracking of almost all pixels. *arXiv preprint arXiv:2512.08358*, 2025. 3

[57] Shunlin Lu, Jingbo Wang, Zeyu Lu, Ling-Hao Chen, Wenxun Dai, Junting Dong, Zhiyang Dou, Bo Dai, and Ruimao Zhang. Scamo: Exploring the scaling law in autoregressive motion generation model. In *Proceedings of the Computer Vision and Pattern Recognition Conference*, pages 27872–27882, 2025. 2

[58] Naureen Mahmood, Nima Ghorbani, Nikolaus F Troje, Gerard Pons-Moll, and Michael J Black. Amass: Archive of motion capture as surface shapes. In *Proceedings of the IEEE/CVF international conference on computer vision*, pages 5442–5451, 2019.

[59] Claire McLean, Makenzie Meendering, Tristan Swartz, Orri Gabbay, Alexandra Olsen, Rachel Jacobs, Nicholas Rosen, Philippe de Bree, Tony Garcia, Gadsden Merrill, et al. Embodiment 3d: A large-scale multimodal motion and behavior dataset. *arXiv preprint arXiv:2510.16258*, 2025. 2

[60] Zichong Meng, Yiming Xie, Xiaogang Peng, Zeyu Han, and Huaizu Jiang. Rethinking diffusion for text-driven human motion generation: Redundant representations, evaluation, and masked autoregression. In *Proceedings of the Computer Vision and Pattern Recognition Conference*, pages 27859–27871, 2025. 2

[61] Hyelin Nam, Hyojun Go, Byeongjun Park, Byung-Hoon Kim, and Hyungjin Chung. Generating human motion videos using a cascaded text-to-video framework. *arXiv preprint arXiv:2510.03909*, 2025. 3

[62] Muyao Niu, Xiaodong Cun, Xintao Wang, Yong Zhang, Ying Shan, and Yinqiang Zheng. Mofa-video: Controllable image animation via generative motion field adaptions in frozen image-to-video diffusion model. In *European Conference on Computer Vision*, pages 111–128. Springer, 2024. 1, 3

[63] Muyao Niu, Mingdeng Cao, Yifan Zhan, Qingtian Zhu, Mingze Ma, Jiancheng Zhao, Yanhong Zeng, Zhihang Zhong, Xiao Sun, and Yinqiang Zheng. Anicrafter: Customizing realistic human-centric animation via avatar-background conditioning in video diffusion models. *arXiv preprint arXiv:2505.20255*, 2025. 3

[64] Boxiao Pan, Zhan Xu, Chun-Hao Huang, Krishna Kumar Singh, Yang Zhou, Leonidas J Guibas, and Jimei Yang. Actanywhere: Subject-aware video background generation. *Advances in Neural Information Processing Systems*, 37: 29754–29776, 2024. 3

[65] Youxin Pang, Yong Zhang, Ruizhi Shao, Xiang Deng, Feng Gao, Xu Xiaoming, Xiaoming Wei, and Yebin Liu. Unimo: Unifying 2d video and 3d human motion with an autoregressive framework. *arXiv preprint arXiv:2512.03918*, 2025. 3

[66] Priyanka Patel and Michael J Black. Camerahmr: Aligning people with perspective. In *2025 International Conference on 3D Vision (3DV)*, pages 1562–1571. IEEE, 2025. 3, 5, 6

[67] Georgios Pavlakos, Vasileios Choutas, Nima Ghorbani, Timo Bolkart, Ahmed AA Osman, Dimitrios Tzionas, and Michael J Black. Expressive body capture: 3d hands, face, and body from a single image. In *Proceedings of the IEEE/CVF conference on computer vision and pattern recognition*, pages 10975–10985, 2019. 3

[68] Huaijin Pi, Ruoxi Guo, Zehong Shen, Qing Shuai, Zechen Hu, Zhumei Wang, Yajiao Dong, Ruizhen Hu, Taku Komura, Sida Peng, et al. Motion-2-to-3: Leveraging 2d motion data to boost 3d motion generation. *arXiv preprint arXiv:2412.13111*, 2024. 2

[69] Matthias Plappert, Christian Mandery, and Tamim Asfour. The kit motion-language dataset. *Big data*, 4(4):236–252, 2016. 2

[70] Abhinanda R Punnakkal, Arjun Chandrasekaran, Nikos Athanasiou, Alejandra Quiros-Ramirez, and Michael J Black. Babel: Bodies, action and behavior with english labels. In *Proceedings of the IEEE/CVF conference on computer vision and pattern recognition*, pages 722–731, 2021. 2

[71] Samyam Rajbhandari, Jeff Rasley, Olatunji Ruwase, and Yuxiong He. Zero: Memory optimizations toward training trillion parameter models. In *SC20: International Conference for High Performance Computing, Networking, Storage and Analysis*, pages 1–16. IEEE, 2020. 5

[72] Joseph Redmon, Santosh Divvala, Ross Girshick, and Ali Farhadi. You only look once: Unified, real-time object detection. In *Proceedings of the IEEE conference on computer vision and pattern recognition*, pages 779–788, 2016. 5, 1, 2

[73] Shenghao Ren, Yi Lu, Jiayi Huang, Jiayi Zhao, He Zhang, Tao Yu, Qiu Shen, and Xun Cao. Motionpro: Exploring the role of pressure in human mocap and beyond. In *Proceedings of the Computer Vision and Pattern Recognition Conference*, pages 27760–27770, 2025. 2

[74] Yiming Ren, Chengfeng Zhao, Yannan He, Peishan Cong, Han Liang, Jingyi Yu, Lan Xu, and Yuexin Ma. Lidar-aid inertial poser: Large-scale human motion capture by sparse inertial and lidar sensors. *IEEE Transactions on Visualization and Computer Graphics*, 29(5):2337–2347, 2023. 5

[75] Robin Rombach, Andreas Blattmann, Dominik Lorenz, Patrick Esser, and Björn Ommer. High-resolution image synthesis with latent diffusion models. In *Proceedings of the IEEE/CVF conference on computer vision and pattern recognition*, pages 10684–10695, 2022. 2

[76] Javier Romero, Dimitrios Tzionas, and Michael J Black. Embodied hands: Modeling and capturing hands and bodies together. *arXiv preprint arXiv:2201.02610*, 2022. 3

[77] Ruizhi Shao, Yinghao Xu, Yujun Shen, Ceyuan Yang, Yang Zheng, Changan Chen, Yebin Liu, and Gordon Wetzstein. Interspatial attention for efficient 4d human video generation. *arXiv preprint arXiv:2505.15800*, 2025. 3

[78] Xiaoyu Shi, Zhaoyang Huang, Fu-Yun Wang, Weikang Bian, Dasong Li, Yi Zhang, Manyuan Zhang, Ka Chun Cheung, Simon See, Hongwei Qin, et al. Motion-i2v: Consistent and controllable image-to-video generation with explicit motion modeling. In *ACM SIGGRAPH 2024 Conference Papers*, pages 1–11, 2024. 3

[79] Guoxian Song, Hongyi Xu, Xiaochen Zhao, You Xie, Tianpei Gu, Zenan Li, Chenxu Zhang, and Linjie Luo. X-unimotion: Animating human images with expressive, unified and identity-agnostic motion latents. *arXiv preprint arXiv:2508.09383*, 2025. 3

[80] Ashkan Taghipour, Morteza Ghahremani, Mohammed Bennamoun, Farid Boussaid, Aref Miri Rekavandi, Zinuo Li, QiuHong Ke, and Hamid Laga. Latentmove: Towards complex human movement video generation. *arXiv preprint arXiv:2505.22046*, 2025. 1, 3

[81] Shuai Tan, Biao Gong, Xiang Wang, Shiwei Zhang, Dandan Zheng, Ruobing Zheng, Kecheng Zheng, Jingdong Chen, and Ming Yang. Animate-x: Universal character image animation with enhanced motion representation. *arXiv preprint arXiv:2410.10306*, 2024. 3

[82] Shuai Tan, Biao Gong, Zhuoxin Liu, Yan Wang, Xi Chen, Yifan Feng, and Hengshuang Zhao. Animate-x++: Universal character image animation with dynamic backgrounds. *arXiv preprint arXiv:2508.09454*, 2025. 3

[83] Joachim Tesch, Giorgio Becherini, Prerana Achar, Anastasios Yiannakidis, Muhammed Kocabas, Priyanka Patel, and Michael J. Black. BEDLAM2.0: Synthetic humans and cameras in motion. In *The Thirty-ninth Annual Conference on Neural Information Processing Systems Datasets and Benchmarks Track*, 2025. 2

[84] Guy Tevet, Sigal Raab, Brian Gordon, Yonatan Shafir, Daniel Cohen-Or, and Amit H Bermano. Human motion diffusion model. *arXiv preprint arXiv:2209.14916*, 2022. 2, 6

[85] Team Wan, Ang Wang, Baole Ai, Bin Wen, Chaojie Mao, Chen-Wei Xie, Di Chen, Feiwu Yu, Haiming Zhao, Jianxiao Yang, et al. Wan: Open and advanced large-scale video generative models. *arXiv preprint arXiv:2503.20314*, 2025. 1, 2, 3, 4, 5, 6, 7, 8

[86] Boyuan Wang, Xiaofeng Wang, Chaojun Ni, Guosheng Zhao, Zhiqin Yang, Zheng Zhu, Muyang Zhang, Yukun Zhou, Xinze Chen, Guan Huang, et al. Humandreamer: Generating controllable human-motion videos via decoupled generation. In *Proceedings of the Computer Vision and Pattern Recognition Conference*, pages 12391–12401, 2025. 3, 5

[87] Haoyu Wang, Hao Tang, Donglin Di, Zhilu Zhang, Wangmeng Zuo, Feng Gao, Siwei Ma, and Shiliang Zhang. Mosa: Motion-coherent human video generation via structure-appearance decoupling. *arXiv preprint arXiv:2508.17404*, 2025. 3

[88] Jiepeng Wang, Zhaoqing Wang, Hao Pan, Yuan Liu, Dongdong Yu, Changhu Wang, and Wenping Wang. Mmgen: Unified multi-modal image generation and understanding in one go. *arXiv preprint arXiv:2503.20644*, 2025. 3

[89] Lizhen Wang, Zhurong Xia, Tianshu Hu, Pengrui Wang, Pengfei Wei, Zerong Zheng, Ming Zhou, Yuan Zhang, and Mingyuan Gao. Dreamactor-h1: High-fidelity human-product demonstration video generation via motion-designed diffusion transformers. *arXiv preprint arXiv:2506.10568*, 2025. 3

[90] QiuHeng Wang, Yukai Shi, Jiarong Ou, Rui Chen, Ke Lin, Jiahao Wang, Boyuan Jiang, Haotian Yang, Mingwu Zheng, Xin Tao, et al. Koala-36m: A large-scale video dataset improving consistency between fine-grained conditions and video content. In *Proceedings of the Computer Vision and Pattern Recognition Conference*, pages 8428–8437, 2025. 5, 1

[91] Ye Wang, Sipeng Zheng, Bin Cao, Qianshan Wei, Qin Jin, and Zongqing Lu. Quo vadis, motion generation? from large language models to large motion models. 2024. 2

[92] Ye Wang, Sipeng Zheng, Bin Cao, Qianshan Wei, Weishuai Zeng, Qin Jin, and Zongqing Lu. Scaling large motion models with million-level human motions. *arXiv preprint arXiv:2410.03311*, 2024. 2

[93] Zhenzhi Wang, Yixuan Li, Yanhong Zeng, Youqing Fang, Yuwei Guo, Wenran Liu, Jing Tan, Kai Chen, Tianfan Xue, Bo Dai, et al. Humanvid: Demystifying training data for camera-controllable human image animation. *Advances in Neural Information Processing Systems*, 37:20111–20131, 2024. 3, 5

[94] Zhenzhi Wang, Yixuan Li, Yanhong Zeng, Yuwei Guo, Dahua Lin, Tianfan Xue, and Bo Dai. Multi-identity human image animation with structural video diffusion. *arXiv preprint arXiv:2504.04126*, 2025. 3

[95] Zhenzhi Wang, Jiaqi Yang, Jianwen Jiang, Chao Liang, Gaojie Lin, Zerong Zheng, Ceyuan Yang, and Dahua Lin. Interacthuman: Multi-concept human animation with layout-aligned audio conditions. *arXiv preprint arXiv:2506.09984*, 2025. 3

[96] Yuxin Wen, Qing Shuai, Di Kang, Jing Li, Cheng Wen, Yue Qian, Ningxin Jiao, Changhai Chen, Weijie Chen,

Yiran Wang, et al. Hy-motion 1.0: Scaling flow matching models for text-to-motion generation. *arXiv preprint arXiv:2512.23464*, 2025. 2

[97] Bize Wu, Jinheng Xie, Meidan Ding, Zhe Kong, Jianfeng Ren, Ruibin Bai, Rong Qu, and Linlin Shen. Finemotion: A dataset and benchmark with both spatial and temporal annotation for fine-grained motion generation and editing. *arXiv preprint arXiv:2507.19850*, 2025. 2

[98] Qi Wu, Yubo Zhao, Yifan Wang, Xinhang Liu, Yu-Wing Tai, and Chi-Keung Tang. Motion-agent: A conversational framework for human motion generation with llms. *arXiv preprint arXiv:2405.17013*, 2024. 2

[99] Dianbing Xi, Jiepeng Wang, Yuanzhi Liang, Xi Qiu, Yuchi Huo, Rui Wang, Chi Zhang, and Xuelong Li. Omnidiff: Omni controllable video diffusion for generation and understanding. *arXiv preprint arXiv:2504.10825*, 2025. 3, 4

[100] Ruihao Xi, Xuekuan Wang, Yongcheng Li, Shuhua Li, Zichen Wang, Yiwei Wang, Feng Wei, and Cairong Zhao. Toward rich video human-motion2d generation. *arXiv preprint arXiv:2506.14428*, 2025. 3

[101] Lixing Xiao, Shunlin Lu, Huajin Pi, Ke Fan, Liang Pan, Yueer Zhou, Ziyong Feng, Xiaowei Zhou, Sida Peng, and Jingbo Wang. Motionstreamer: Streaming motion generation via diffusion-based autoregressive model in causal latent space. In *Proceedings of the IEEE/CVF International Conference on Computer Vision (ICCV)*, pages 10086–10096, 2025. 2

[102] Weitao Xiong, Zhiyuan Yuan, Jiahao Lu, Chengfeng Zhao, Peng Li, and Yuan Liu. Huprior3r: Incorporating human priors for better 3d dynamic reconstruction from monocular videos. *arXiv e-prints*, pages arXiv–2512, 2025. 3

[103] Yufei Xu, Jing Zhang, Qiming Zhang, and Dacheng Tao. Vitpose: Simple vision transformer baselines for human pose estimation. *Advances in neural information processing systems*, 35:38571–38584, 2022. 1, 2

[104] An Yang, Baosong Yang, Beichen Zhang, Binyuan Hui, Bo Zheng, Bowen Yu, Chengyuan Li, Dayiheng Liu, Fei Huang, Haoran Wei, Huan Lin, Jian Yang, Jianhong Tu, Jianwei Zhang, Jianxin Yang, Jiaxi Yang, Jingren Zhou, Junyang Lin, Kai Dang, Keming Lu, Keqin Bao, Kexin Yang, Le Yu, Mei Li, Mingfeng Xue, Pei Zhang, Qin Zhu, Rui Men, Runji Lin, Tianhao Li, Tingyu Xia, Xingzhang Ren, Xuancheng Ren, Yang Fan, Yang Su, Yichang Zhang, Yu Wan, Yuqiong Liu, Zeyu Cui, Zhenru Zhang, and Zihan Qiu. Qwen2.5 technical report. *arXiv preprint arXiv:2412.15115*, 2024. 5, 1

[105] An Yang, Anfeng Li, Baosong Yang, Beichen Zhang, Binyuan Hui, Bo Zheng, Bowen Yu, Chang Gao, Chen-gen Huang, Chenxu Lv, Chujie Zheng, Dayiheng Liu, Fan Zhou, Fei Huang, Feng Hu, Hao Ge, Haoran Wei, Huan Lin, Jialong Tang, Jian Yang, Jianhong Tu, Jianwei Zhang, Jianxin Yang, Jiaxi Yang, Jing Zhou, Jingren Zhou, Junyang Lin, Kai Dang, Keqin Bao, Kexin Yang, Le Yu, Lianghao Deng, Mei Li, Mingfeng Xue, Mingze Li, Pei Zhang, Peng Wang, Qin Zhu, Rui Men, Ruize Gao, Shixuan Liu, Shuang Luo, Tianhao Li, Tianyi Tang, Wenbiao Yin, Xingzhang Ren, Xinyu Wang, Xinyu Zhang, Xuancheng Ren, Yang Fan, Yang Su, Yichang Zhang, Yinger Zhang, Yu Wan, Yuqiong Liu, Zekun Wang, Zeyu Cui, Zhenru Zhang, Zhipeng Zhou, and Zihan Qiu. Qwen3 technical report. *arXiv preprint arXiv:2505.09388*, 2025. 5, 1, 2, 3

[106] Yuxiao Yang, Hualian Sheng, Sijia Cai, Jing Lin, Jiahao Wang, Bing Deng, Junzhe Lu, Haoqian Wang, and Jieping Ye. Echomotion: Unified human video and motion generation via dual-modality diffusion transformer. *arXiv preprint arXiv:2512.18814*, 2025. 3

[107] Zhendong Yang, Ailing Zeng, Chun Yuan, and Yu Li. Effective whole-body pose estimation with two-stages distillation. In *Proceedings of the IEEE/CVF International Conference on Computer Vision*, pages 4210–4220, 2023. 3, 8

[108] Zhuoyi Yang, Jiayan Teng, Wendi Zheng, Ming Ding, Shiyu Huang, Jiazheng Xu, Yuanming Yang, Wenyi Hong, Xiaohan Zhang, Guanyu Feng, et al. Cogvideox: Text-to-video diffusion models with an expert transformer. *arXiv preprint arXiv:2408.06072*, 2024. 1, 2, 7

[109] Jianrong Zhang, Yangsong Zhang, Xiaodong Cun, Yong Zhang, Hongwei Zhao, Hongtao Lu, Xi Shen, and Ying Shan. Generating human motion from textual descriptions with discrete representations. In *Proceedings of the IEEE/CVF conference on computer vision and pattern recognition*, pages 14730–14740, 2023. 2

[110] Lvmin Zhang, Anyi Rao, and Maneesh Agrawala. Adding conditional control to text-to-image diffusion models. In *Proceedings of the IEEE/CVF international conference on computer vision*, pages 3836–3847, 2023. 1, 2, 4

[111] Mingyuan Zhang, Xinying Guo, Liang Pan, Zhongang Cai, Fangzhou Hong, Huirong Li, Lei Yang, and Ziwei Liu. Remodiffuse: Retrieval-augmented motion diffusion model. In *Proceedings of the IEEE/CVF International Conference on Computer Vision*, pages 364–373, 2023. 2

[112] Yuang Zhang, Jiaxi Gu, Li-Wen Wang, Han Wang, Junqi Cheng, Yuefeng Zhu, and Fangyuan Zou. Mimicmotion: High-quality human motion video generation with confidence-aware pose guidance. *arXiv preprint arXiv:2406.19680*, 2024. 1, 3

[113] Chengfeng Zhao, Juze Zhang, Jiashen Du, Ziwei Shan, Junye Wang, Jingyi Yu, Jingya Wang, and Lan Xu. I’m hoi: Inertia-aware monocular capture of 3d human-object interactions. In *Proceedings of the IEEE/CVF Conference on Computer Vision and Pattern Recognition*, pages 729–741, 2024. 5

[114] Dian Zheng, Ziqi Huang, Hongbo Liu, Kai Zou, Yinan He, Fan Zhang, Yuanhan Zhang, Jingwen He, Wei-Shi Zheng, Yu Qiao, and Ziwei Liu. VBench-2.0: Advancing video generation benchmark suite for intrinsic faithfulness. *arXiv preprint arXiv:2503.21755*, 2025. 2, 5, 7

[115] Jingkai Zhou, Benzhi Wang, Weihua Chen, Jingqi Bai, Dongyang Li, Aixi Zhang, Hao Xu, Mingyang Yang, and Fan Wang. Realisdance: Equip controllable character animation with realistic hands. *arXiv preprint arXiv:2409.06202*, 2024. 1, 3

[116] Jingkai Zhou, Yifan Wu, Shikai Li, Min Wei, Chao Fan, Weihua Chen, Wei Jiang, and Fan Wang. Realisdance-dit: Simple yet strong baseline towards controllable character

animation in the wild. *arXiv preprint arXiv:2504.14977*, 2025. [1](#), [3](#)

[117] Wenyang Zhou, Zhiyang Dou, Zeyu Cao, Zhouyingcheng Liao, Jingbo Wang, Wenjia Wang, Yuan Liu, Taku Komura, Wenping Wang, and Lingjie Liu. Emdm: Efficient motion diffusion model for fast and high-quality motion generation. In *European Conference on Computer Vision*, pages 18–38. Springer, 2024. [2](#)

[118] Shenhao Zhu, Junming Leo Chen, Zuozhuo Dai, Zilong Dong, Yinghui Xu, Xun Cao, Yao Yao, Hao Zhu, and Siyu Zhu. Champ: Controllable and consistent human image animation with 3d parametric guidance. In *European Conference on Computer Vision*, pages 145–162. Springer, 2024. [1](#), [3](#)

CoMoVi: Co-Generation of 3D Human Motions and Realistic Videos

Supplementary Material

A. More Implementation Details

The main paper outlines the primary training and experimental parameters. This section provides a comprehensive description of multiple stages of our model training, and the detailed procedures for the comparative experiments on motion and video generation tasks.

Training. Our model training is conducted in two stages. The first stage adapts the copied motion DiT branch $\mathcal{D}^{\text{motion}}$ to our 2D motion representation domain using $\mathcal{L}^{\text{motion}}$ only. During this stage, only $\mathcal{D}^{\text{motion}}$ is enabled with gradient calculation and weight update, trained for 2,000 steps. In the second stage, we incorporate the mutually interactive zero-linear layers and 3D-2D cross-attention modules into the training process, using the total loss \mathcal{L} to supervise it. To enhance training efficiency and reduce GPU memory consumption, at each training step we randomly select the latent features from three DiT layers, while consistently including the final layer of $\mathcal{D}^{\text{video}}$ and $\mathcal{D}^{\text{motion}}$, to operate feature fusion and perform cross-attention with the 3D motion query. The pre-trained weights of RGB DiT branch $\mathcal{D}^{\text{video}}$ are frozen, while the remaining components are updated over 4,000 steps at the second training stage. In total, the model is trained for 6,000 steps across both stages. Detailed hyperparameter configurations are provided in Tab. 1.

Experiments of Motion Generation. For 3D human motion evaluation, we follow the 263-dimensional representation and use the pretrained motion and text encoder provided by HumanML3D [20]. The metrics reported in the main paper are determined by the average of 20 independent inference results with a confidence interval of 95% for each model.

Experiments of Video Generation. For fair comparative experiments of video generation task, all models are evaluated at their optimal resolutions (768×1360 for CogVideoX1.5-I2V-5B [108], and 704×1280 for Wan2.2-I2V-5B [85] and ours), and each model is configured to generate video sequences of a unified length of 81 frames. All results are generated once using random seed 42 and CFG scale 6.0 without any cherry-picking.

B. CoMoVi Dataset Curation

In the main paper, we give an overview of our dataset construction process. Here, we elaborate on the detailed procedures. As illustrated in Fig. 1, firstly, we curate a collection of high-quality videos sourced from the Internet and the Koala-36M dataset [90], and employ LLMs/VLMs [104, 105] to selectively retain only those depicting

Hyper-parameter	Value
Batch Size / GPU	1 / 24
Accumulate Step	4
Optimizer	AdamW
Weight Decay	3e-2
Learning Rate	2e-5
AdamW β_1	0.9
AdamW β_2	0.999
Learning Rate Schedule	Constant with Warmup
Warmup Steps	100
Training Steps	6,000
Resolution	704×1280
Max Gradient Norm	0.5
Weighting Scheme	Uniform
Pre-trained Model	Wan2.2-I2V-5B
Sampler	Flow Unipc
Sample Steps	50
CFG Scale	6.0
Training Device	A100-SXM4-40G $\times 24$
Training Strategy	ZeRO-3
Gradient Checkpointing	True
CPU Offload	True
Precision	bf16
Training Speed	280s per accumulation
Inference Speed	15min per video in 5s

Table 1. Hyper-parameters of our model training and inference.

single-person movements (Sec. B.1). Subsequently, we apply 2D human pose detection model [72, 103] to filter out videos where the subject is largely outside the frame or severely occluded (Sec. B.2). The filtered videos are finally captioned (Sec. B.3) and labeled with 3D motion (Sec. B.4). We provide specific prompt instructions used at each filtering stage and our confirmation of dataset ethics (Sec. B.5) below.

B.1. Multimodal Video Filtering

Given a large collection of publicly available videos, we ask the Qwen3 model [105] to determine if the video contents satisfy our criteria according to the corresponding dense captions using the prompt instruction shown in Fig. 2. We only keep the videos that are judged as “[‘Yes’, ‘Yes’, ‘Yes’, ‘Yes’]” in this initial text-based filtering stage, and then process them using the Qwen2.5-VL model [104], which takes the first frame of each video and the prompt instruction specified in Fig. 3 to make a visual confirmation. This multimodal filtering procedure effectively filters out non-human videos, multi-person videos, and contents such as movies,

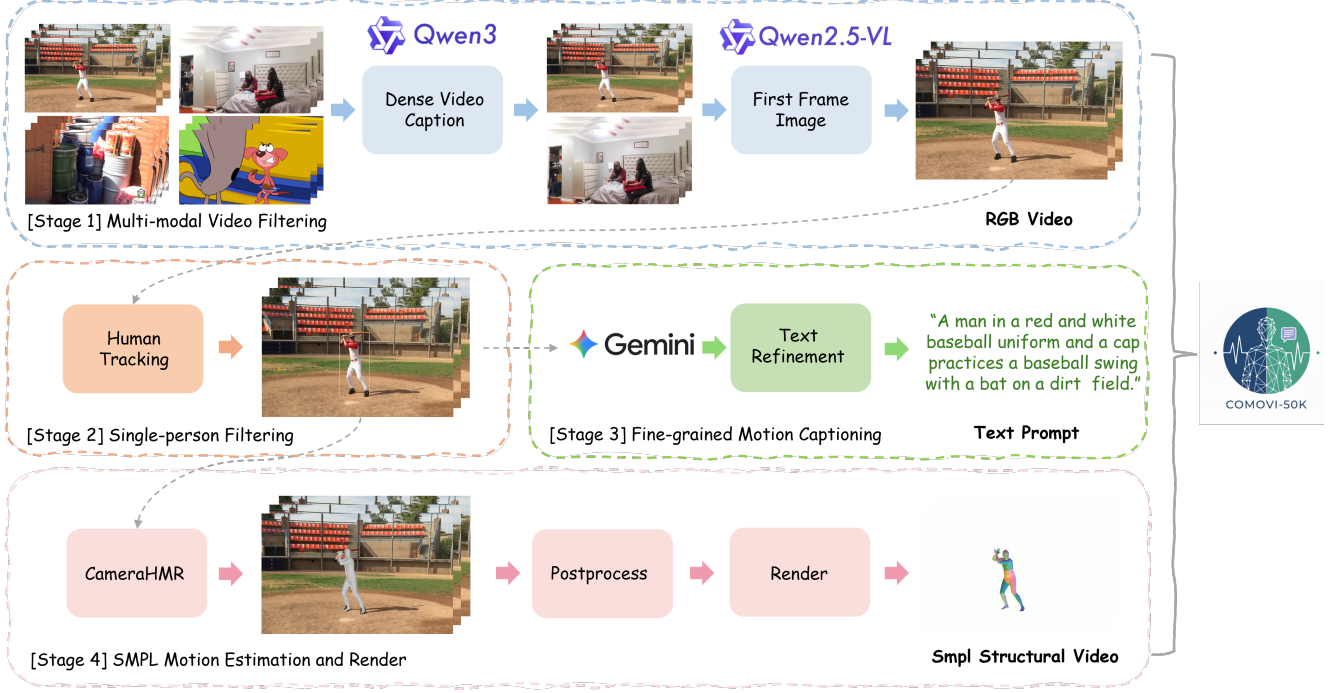


Figure 1. Curation pipeline of our CoMoVi Dataset.

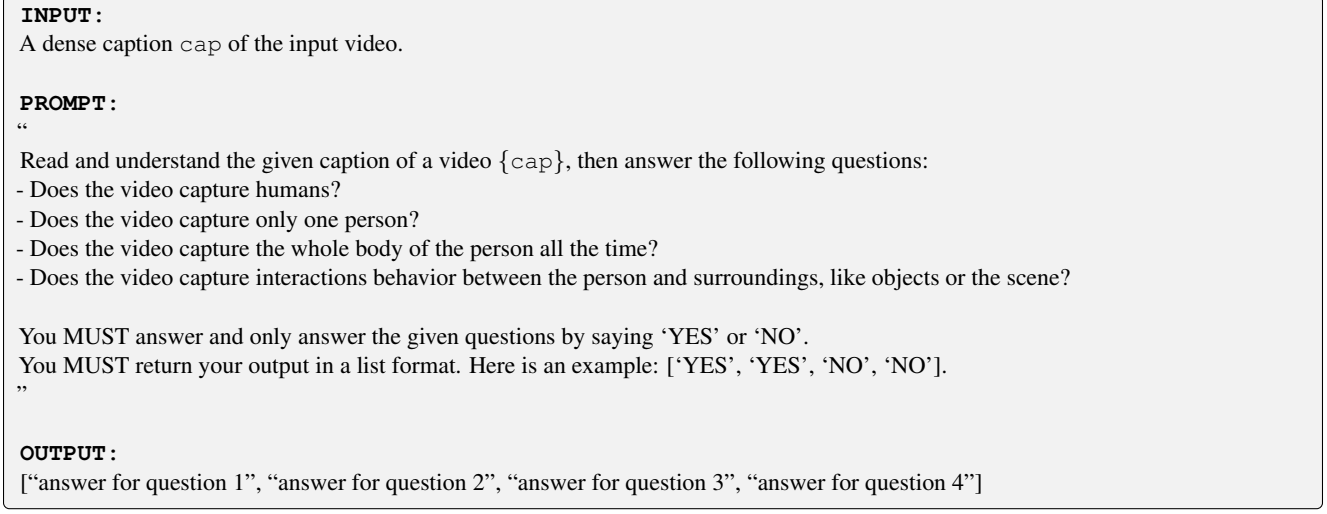


Figure 2. Prompt instruction for Qwen3 [105] to analyze dense video captions.

animations, and video games that may contain human-like characters but do not represent real-world human motions.

B.2. Human Tracking Filtering

To ensure a balanced data distribution and avoid overwhelming clips from long videos, we segment each video into non-overlapping 5-second clips, with a maximum of two clips retained per video. Subsequently, we apply human tracking utilizing YOLO [72] and ViTPose [103] for each clip. A series of confidence thresholds are established to flag frames with low-confidence human detections throughout

a sequence. Clips containing an excessive number of such low-confidence frames are filtered out to ensure data quality.

B.3. Video Captioning

For all retained 5-second clips, the human motion captioning is performed by querying the Gemini-2.5-Pro API at 1 fps, adhering to the official recommendation. The prompt instruction provided for motion captioning is shown in Fig. 4. We also experiment with higher frame rates, which do not yield improvement in caption quality but substantially increase the cost of annotation.

INPUT:
The first frame `frame` of the input video.

PROMPT:

“

You will be given the image `{frame}`, answer ‘YES’ if and only if the following conditions are met:

- There exists one and only one human in this image.
- The human is not a child.
- The whole body of the human is visible in the image, from head to feet.
- The human is not giving a talk, interview, presentation or speech.
- The image is not a game, television, movie, anime or cartoon screen.

Otherwise, answer ‘NO’.

Remember, you MUST only answer ‘YES’ or ‘NO’.

”

OUTPUT:
‘YES’ or ‘NO’

Figure 3. Prompt instruction for Qwen2.5-VL [105] to analyze the first frame of video.

INPUT:
A video `video`.

PROMPT:

“

You will be shown a human video `{video}`. You should identify the most prominent subject in this video and describe the appearance and motion of that person only, ignore other people. You should also describe the objects interacting with or near to the human if any. Don’t use plural words like ‘they/their/them’, start your description with ‘A/The person/man/male/boy/woman/female/girl’. If you use the word ‘left’ or ‘right’, ‘forward’ or ‘backward’, you should always describe it relative to the person’s body, not the camera or screen.

You are required to return a short caption of `{video}`. Give a brief and accurate description of the human appearance, clothing, and motion in only one sentence. Describe the appearance and clothing first and then the motion with possible interactions with surrounding objects. Use the specific and proper terms to describe the motion whenever possible.

”

OUTPUT:

A short caption.

Figure 4. Prompt instruction for Gemini2.5-Pro to caption human motion in videos.

B.4. 3D Human Motion Annotation

We estimate the SMPL parameters [54] for each frame of the filtered human videos using CameraHMR [66]. Since these per-frame estimations are independent, which can lead to motion jitter due to occlusions or motion blur in videos, we apply the smoothing curve in Blender to post-process the estimated body motions to ensure temporal coherence. For consistency of body shape across the video sequence, the SMPL shape parameters estimated from the first frame are applied to all subsequent frames.

B.5. Dataset Ethics

We strictly adhere to the conference ethics guidelines and only collect publicly available videos from academic datasets and open social media platforms. We confirm that all collected data are used only for research purposes. This condition will also be explicitly stated upon the release of our

dataset. We fully respect the privacy of the individuals appearing in the videos, so no personal information or metadata is retained. Furthermore, in compliance with video ownership rights, only video identifiers will be publicly released, rather than the original video files.

C. Limitations and Future Work

While our method offers significant advantages, it is constrained to generating fixed-length motion sequences, lacking the capacity for variable-length or infinite-length generation. Additionally, due to the inherently denser nature of video latents compared to 3D human motion data, our inference speed is relatively slower. Promising future directions include extending our framework to human-object interaction scenarios, employing distillation techniques for generation acceleration, and enabling the generation of variable-length sequences.